Bayesian sensitivity analysis of flight parameters that affect main landing gear yield locations

P. Sartor
pia.sartor@bristol.ac.uk
Department of Aerospace Engineering
University of Bristol
Bristol
UK

K. Worden
k.worden@shefield.ac.uk
Department of Mechanical Engineering
University of Sheffield
Sheffield
UK

R. K. Schmidt
kyle.schmidt@safranmbd.com
D. A. Bond
david.bond@safranmbd.com
Messier-Bugatti-Dowty
Gloucester
UK

ABSTRACT

An aircraft and landing gear loads model was developed to assess the Margin of Safety (*MS*) in main landing gear components such as the main fitting, sliding tube and shock absorber upper diaphragm tube. Using a technique of Bayesian sensitivity analysis, a number of flight parameters were varied in the aircraft and landing gear loads model to gain an understanding of the sensitivity of the MS of the main landing gear components to the individual flight parameters in symmetric two-point landings. The significant flight parameters to the main fitting *MS*, sliding tube bending moment *MS* and shock absorber upper diaphragm tube *MS* include: longitudinal tyre-runway friction coefficient, aircraft vertical descent velocity, aircraft Euler pitch angle and aircraft mass. It was also shown that shock absorber servicing state and tyre pressure do not contribute significantly to the *MS*.

Paper No. 4126. Manuscript received 12 January 2014, accepted 16 June 2014.

https://doi.org/10.1017/S0001924000010150 Published online by Cambridge University Press

NOMENCLATURE

CG	aircraft Centre of Gravity
DOE	Design of Experiments
GP	Gaussian Process
mass	aircraft mass
MEI	Main Effects Indices
MLG	Main Landing Gear
MS	Margin of Safety
Port SA	Port main landing gear servicing state
RMS	Root Mean Square
SAT	Shock Absorber Travel
TEI	Total Effects Indices
tyre	tyre type
tyre press	tyre pressure
V_{A_x}	aircraft longitudinal velocity
V_{A_z}	aircraft vertical descent velocity
θ	aircraft Euler pitch angle
μ_{long}	longitudinal tyre-runway friction coefficient
σ^2	emulator variance

1.0 INTRODUCTION

The landing gear of an aircraft is a unique component as it must bear extreme and varying loads when an aircraft manoeuvres on the ground or lands, yet it must be lightweight and compact so that it can be stowed during flight. The landing gear is both a structure and machine. In its simplest form, it is a structure with energy absorption capability. However, in its modern incarnation it is a complex machine with controlled articulation, multiple axes of energy absorption, and the sole structure supporting the aircraft when on the ground[1].

In most applications, landing gear have no structural redundancy. This, coupled with the conflicting design requirements of high load carrying capacity versus minimum weight and size, results in a landing gear being predominantly manufactured from very high strength (but relatively low toughness) steel, aluminum, and titanium alloys. This is in contrast to most airframes and other metallic aircraft structures, which are typically made from ductile aluminum alloys that are more damage tolerant.

The significant difference between the aircraft structure and landing gear is also reflected in the fact that aircraft design and approval philosophies are quite different between the airframe structure and the landing gear. For example, modern airframe designs use a ‘damage tolerant’ design philosophy, which assumes that cracks exist in the structure and the structure is designed to retain adequate strength until the crack is detected and corrective action is taken[2]. Landing gear however, use a ‘safe life’ design philosophy in which the component is designed to a specific crack-free service life and is removed from service before this elapsed time so that the probability of failure is extremely remote. This is because in high strength materials, crack growth is very rapid and critical crack sizes may not be detectable.

Since the landing gear is the sole structure supporting the aircraft on the ground and damage beyond that assumed in safe life calculations is not accounted for, landing gear overloads are a significant interest for operators, aircraft manufacturers and landing gear manufacturers[3].

https://doi.org/10.1017/S0001924000010150 Published online by Cambridge University Press

A landing gear overload occurs when the landing gear has exceeded its structural capability, which is defined by its static structural capability and its fatigue structural capability.

The static structural capability of the landing gear is the load or combination of loads that it can carry without reaching the material yield point at some location. Material which has exceeded its yield point[†] may be left with residual stress, which can lead to a stress corrosion cracking failure or a fatigue initiated landing gear failure, at a load less than the static limit load.

The serviceability of the landing gear structure is based on a loading Margin of Safety (*MS*), which in this paper is the ratio of the allowable load, defined by the material yield point, to the actual load, minus one. The landing gear components are considered serviceable if the *MS* is greater than zero because there is no yielding of the component material sufficient to produce residual stress of a magnitude that will affect the fatigue life.

In this paper, an aircraft and landing gear dynamic model has been developed to assess how the aircraft and landing gear flight parameters affect the *MS* at several locations on the Main Landing Gear (MLG) structure. Using a technique of Bayesian sensitivity analysis, a number of flight parameters, such as aircraft Euler pitch angle, aircraft longitudinal velocity, vertical descent velocity, longitudinal tyre-runway friction coefficient, MLG shock absorber servicing state (i.e. correct fluid volume and gas pressure), tyre type, tyre pressure, aircraft mass and aircraft centre of gravity location, are varied in the aircraft and landing gear model to gain an understanding of how the model responds to variations in the inputs, to identify the most influential input parameters and to identify which input parameters have little or no effect on the *MS*[4]. In this technique, an emulator of the model is created by fitting a Gaussian Process (GP) to a response surface using data from multiple runs of the model as dictated by a Design of Experiments (DOE) so that the output of the model can be predicted for any point in the input space without having to run the simulation. Each input parameter is represented as a probability distribution and sensitivity analysis data is inferred at a reduced computational cost and with little loss of accuracy[5,6].

This paper first describes the loads of interest when determining the serviceability of the MLG structure. The aircraft and landing gear dynamic model is then explained. A brief background of the Bayesian sensitivity analysis is then presented. Finally, the results of the sensitivity analysis for symmetric landings using the aircraft and landing gear model are shown.

2.0 LANDING GEAR LOADS

Figure 1 illustrates a typical aircraft structure and Fig. 2 shows a typical telescopic, cantilever port MLG structure, with the sign conventions used in this paper. The MLG structure consists of the following components: the main fitting and forward and rear pintle pins, which provides housing for the upper part of the shock absorber and forms part of the attachment to the aircraft structure; the sliding tube and axle, which are one machined component that form the bottom part of the shock absorber; the torque links, which maintain the alignment of the axle; the sidestay, which acts in the forward and side planes to prevent sideways movement of the landing gear and also forms an attachment to the aircraft structure; and the retraction actuator, which allows for extension and retraction of the landing gear.

The shock absorber is a two-stage, oleo-pneumatic device as shown in Fig. 3. The first stage contains both hydraulic fluid and low pressure nitrogen gas, while the second stage contains only high pressure nitrogen gas. The hydraulic fluid in the first stage is separated from the gas in the second stage by a separator piston.

[†] The yield point of a material is normally defined at 0·2% strain. However, yield, and therefore residual stress, may occur in the component at any point beyond the proportional limit.

https://doi.org/10.1017/S0001924000010150 Published online by Cambridge University Press

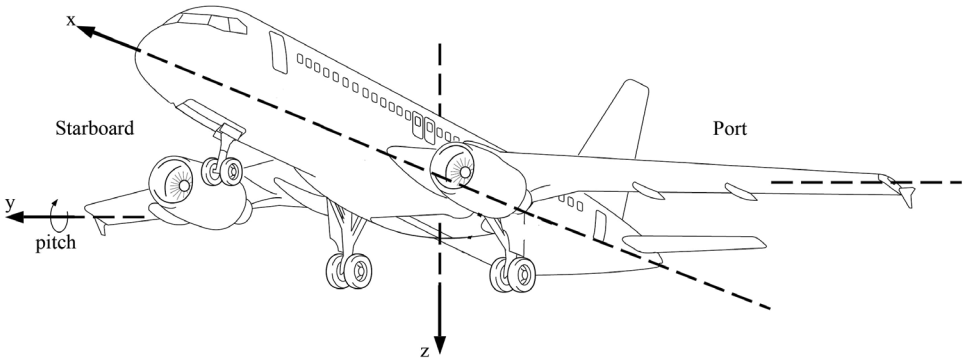


Figure 2. Typical main landing gear structure with sign convention.

During shock absorber compression on landing, the compression chamber is forced up and the oil is transferred to the gas chamber through a variable area orifice generating a pressure differential. The volume of the shock absorber is reduced and the increasing fluid pressure causes the separator piston to compress the gas in the second stage. Fluid is also transferred from the gas chamber into the recoil chamber. The compression of gas and the fluid transfer in the first stage, and the gas compression in the second stage generates spring and damping loads which are a function of shock absorber travel (SAT) and stroke velocity. As the compression stroke ends, the energy stored in the compressed gas initiates the recoil stroke. The gas pressure in the second stage moves the separator piston to force the fluid back. Fluid is forced to return via the recoil orifice plates, which slows the fluid flow and therefore damps the recoil stroke.

Figure 4 illustrates the landing dynamics of the port MLG in a two-point, symmetric landing. The starboard MLG landing dynamics are identical to the port MLG in a symmetric landing. On approach, the landing gear wheels are not spinning, however, on contact with the runway, the landing gear wheels spin-up to the ground speed of the aircraft under the influence of the ground reaction and the tyre-runway friction. The resulting drag force deforms the landing gear aft and

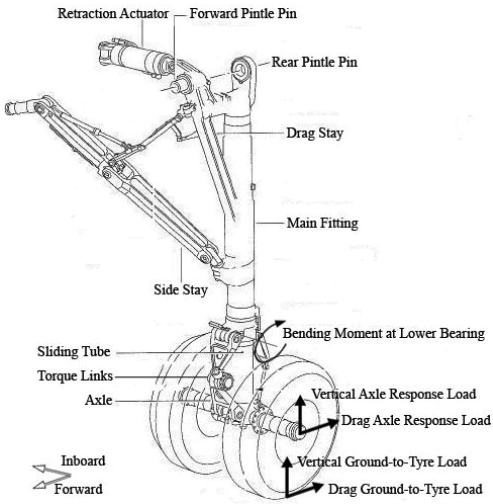


Figure 2. Typical main landing gear structure with sign convention.

https://doi.org/10.1017/S0001924000010150 Published online by Cambridge University Press

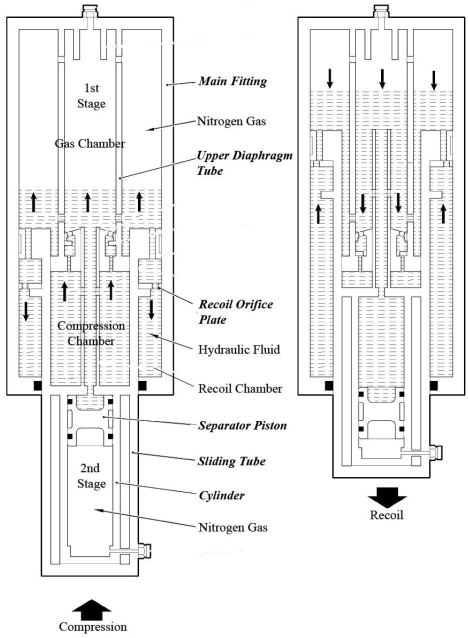


Figure 3. Two-stage shock absorber.

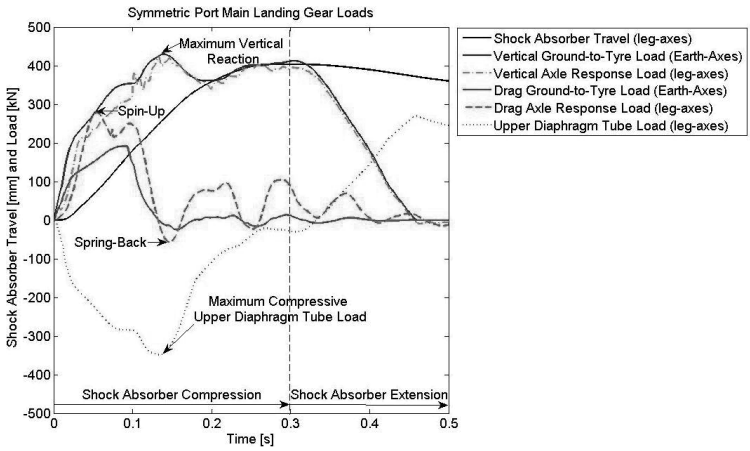


Figure 4. Example of symmetric port main landing gear landing dynamics.

stores energy in the structure. When the tyre velocity reaches the aircraft forward speed, the frictional force between the tyre and the ground reduces and the release of the strain energy stored in the rearward deformation produces a spring-back. The landing gear oscillates until the structural damping reduces the stored energy to zero[7]. Also during this time, there is an increasing vertical ground-to-tyre load, which is a function of the gas spring, oil damping (related to the square of the vertical descent velocity) and bearing friction. The shock absorber travel (SAT), in conjunction with the landing loads, creates a bending moment on the landing gear structure which is computed at the lower bearing. There are no side ground-to-tyre loads developed in a symmetric landing.

https://doi.org/10.1017/S0001924000010150 Published online by Cambridge University Press

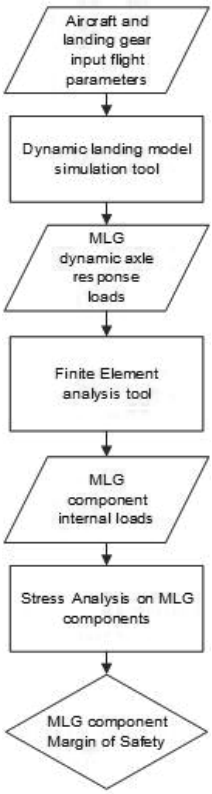


Figure 5. Overview of the aircraft and landing gear loads model.

In order to calculate the internal landing gear loads and to assess the serviceability of the landing gear structure after a landing, the axle response loads are required. The ground-to-tyre loads, discussed previously, act as the forcing function, which combined with the mass and flexibility characteristics of the landing gear, produce the dynamic response loads at the landing gear axle. The difference between the ground-to-tyre loads and the axle dynamic response loads is due to the inertial forces of the landing gear mass between the ground and the landing gear axle during the impact[8].

A landing gear internal loads analysis is performed to calculate the loads in each component of the landing gear structure. Using the internal loads, stress analysis is then performed to determine whether any of the landing gear components have detrimentally yielded.

3.0 OVERVIEW OF THE AIRCRAFT AND LANDING GEAR LOADS MODEL

The aircraft and landing gear loads model consists of: (1) a Fortran dynamic landing model simulation tool, (2) a Finite Element (FE) analysis internal loads tool and (3) conversion of loads to local component stresses. An overview of the model is presented in Fig. 5. The dynamic landing model simulation tool is used to simulate symmetric landings based on the aircraft and landing gear flight parameters. The landing gear dynamic axle response loads and corresponding SAT at spin-up, spring-back and maximum vertical reaction are then used in the Finite Element analysis beam model tool to perform static analysis on the landing gear so that the MLG component internal loads and moments can be calculated. Finally, using these loads and moments, a stress analysis of each component is performed to determine whether it has detrimentally yielded.

The landings are simulated using a Fortran dynamic landing model simulation tool, which allows the user to formulate aircraft and landing gear models and solve the aircraft and landing gear equations of motion for symmetric landings to obtain tabulated time histories of displacements, velocities, accelerations, forces and moments. In the model, the aircraft and landing gear are represented by a number of mass systems, including the aircraft-less-landing gear, each landing gear and the wheels. Each landing gear is connected to the aircraft-less-landing gear system by springs and dampers represented by attachment stiffness and damping matrices. By representing the whole aircraft in this way, each mass system can be treated independently.

The aircraft is represented as a 6-DoF rigid body with mass, inertia, centre of gravity (CG) and aerodynamic data. The telescopic, cantilever landing gear is comprised of the main fitting and sliding tube which move relative to each other, and contains a two-stage shock absorber, as described in Section 2. The flexible MLG model includes the landing gear geometry, structural, modal, shock absorber and attachment data. The wheel data include the radial force, normal force, cornering power and self-aligning torque. The wheel systems have wheel rotational freedoms.

The forces and moments that act on the aircraft system include gravity, aerodynamic forces, thrust and the aircraft to landing gear attachment reaction forces. Forces and moments that act on the landing gear leg systems come from the tyre-to-ground contact and the aircraft to landing gear

https://doi.org/10.1017/S0001924000010150 Published online by Cambridge University Press

attachments. The shock absorber gas, hydraulic and friction forces are a function of the SAT and external forces acting on the landing gear leg. The link between the aircraft and leg systems comes from the attachment forces which result from the displacement between the attachment locations on the landing gear leg and the aircraft. Using the initial conditions for the simulation, the system of differential equations representing the aircraft, landing gear and wheel equations of motion are solved using a Runge-Kutta integration process. The Fortran dynamic model simulation tool was verified using landing gear drop test data as well as available dynamic landing simulation results from a model that was verified using flight test data.

A landing gear internal loads analysis is then performed by running the landing gear dynamic axle response loads through a finite element analysis tool to perform static analysis on the landing gear to calculate the component internal loads and moments. Each component of the landing gear is represented by a beam element with representative section and material properties. The beams are joined by spring joints to give the correct degrees of freedom. The finite element model is analysed using a non-linear iterative process so that the effects of deflections are included in the internal loads analysis. The internal load outputs are given for the main fitting and sliding tube bending moment. The shock absorber upper diaphragm tube load due to the hydraulic damping is also calculated from the dynamic landing simulation.

Using the internal loads from the beam model, stress analysis is then performed to determine whether the components have detrimentally yielded. The landing gear component *MS* is determined by:

$$Margin\ of\ Safety\ (MS) = \frac{Allowable\ Load}{Actual\ Load} - 1 \qquad \ldots (1)$$

Components are considered serviceable if the $MS > 0$.

4.0 MARGIN OF SAFETY SENSITIVITY ANALYSIS

Any computer model, such as the aircraft and landing gear loads model, can be considered to be a function of its inputs. Although this function is deterministic and governed by known mathematical functions, it is often complex and may actually be encoded by a large numerical model which has no closed-form expression for its outputs as a function of its inputs. Therefore, this function could be considered unknown, since the output is unknown for a given set of inputs until the model has actually been run. If however, the function (model) is sampled at a number of carefully chosen input points, it is possible to fit a response surface which can predict the output of the model for any point in the input space without having to run the model. For models that are computationally expensive, creating an emulator (a model of a model) is a useful approach for sensitivity analysis which generally requires multiple runs of the model under investigation[5]. A particular probabilistic approach for developing an emulator is the use of Gaussian Process (GP) regression[9-11]. Using this emulator, it is then possible to infer sensitivity analysis data at a reduced computational cost and with little loss of accuracy. Computational savings can be up to two orders of magnitude compared to using a Monte Carlo method[5,12]. The full details of the GP emulator and the sensitivity analysis measures can be found in Refs 5,13,14. The sensitivity analysis presented in this paper was conducted using the software package Gaussian Emulation Machine for Sensitivity Analysis (GEM-SA)[15].

Using the Bayesian sensitivity analysis technique, a number of flight parameters are varied in the aircraft and landing gear loads model, described in Section 3, to gain an understanding of the sensitivity of the MLG component yield locations to the input flight parameters. While the Bayesian

https://doi.org/10.1017/S0001924000010150 Published online by Cambridge University Press

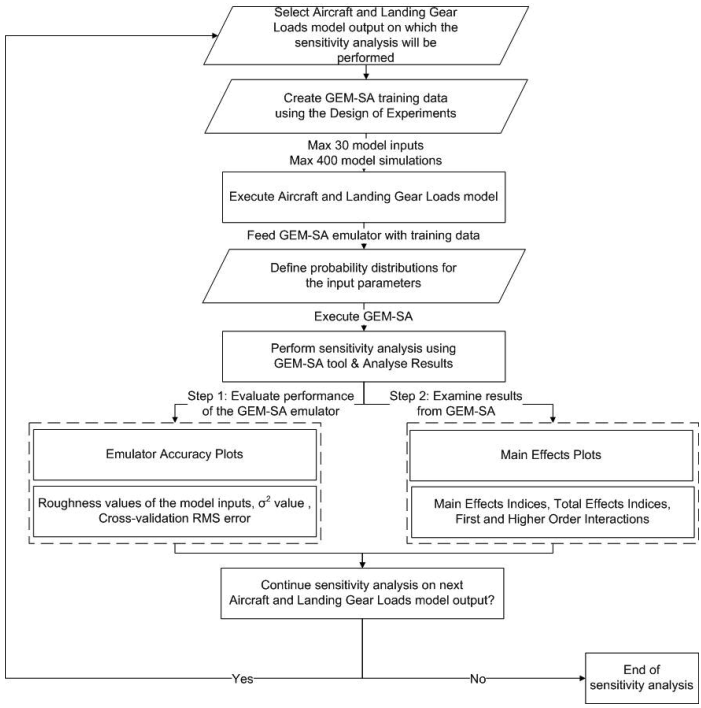


Figure 6. Methodology followed in conducting the sensitivity analysis on the aircraft and landing gear.loads model using GEM-SA, after Ref. 16.

sensitivity analysis technique has been used to examine the sensitivity of models in a variety of disciplines including: soil-vegetation-atmospheric transfer[16], nuclear radiation releases[10], vehicle crash, spot welding[17] and the aortic valve[18], this is a novel application of the Bayesian sensitivity analysis technique to an aircraft landing gear model.

Figure 6 provides a summary of the methodology followed in conducting the sensitivity analysis on the aircraft and landing gear loads model using GEM-SA in this paper. The Bayesian sensitivity analysis technique in GEM-SA is comprised of two stages: the first involves creating an emulator of the aircraft and landing gear loads model by fitting a GP to the response surface using data from multiple runs of the model as dictated by a Design of Experiments (DOE) so that the output of the model can be predicted for any point in the input space without having to run the simulation. The second stage involves representing each input flight parameter as a probability distribution and using the emulator built in the first stage to infer sensitivity analysis data such as Main Effects plots, Main Effects Indices (MEI), Total Effects Indices (TEI), first order interactions and higher order interactions.

For symmetric, two-point landings, the nine input flight parameters to the aircraft and landing gear loads model include: aircraft Euler pitch angle (θ), aircraft longitudinal velocity (V_{A_x}), vertical descent velocity (V_{A_z}), longitudinal tyre-runway friction coefficient (μ_{long}), MLG shock absorber servicing state (*Port SA*[†]), tyre type (*tyre*), tyre pressure (*tyre press*), aircraft mass (*mass*) and aircraft centre of gravity location (*CG*).

In order to estimate the sensitivity measures described previously, the probability distributions for the input parameters are defined. In reality flight parameters such as pitch and ground speed are not independent however, given the limited range considered at landing, they have been considered

[†] For symmetric landings, the starboard MLG mirrors the port MLG therefore only the port MLG servicing state is specified.

https://doi.org/10.1017/S0001924000010150 Published online by Cambridge University Press

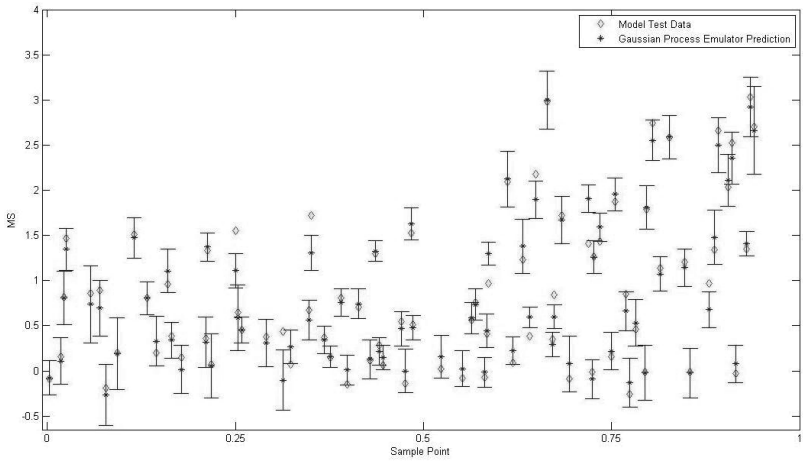


Figure 7. Symmetric landing spin-up main fitting emulator accuracy measures.

independent for the purpose of this investigation. The parameters can be specified as either Gaussian or uniform distributions based on how informative the available input parameter data are. In this study, the distributions have been defined as uniform distributions and the ranges of the flight parameters, normalised between zero and one, are based on typical aircraft operating limitations.

To develop the emulator, 400 combinations of input parameters were generated using a maximin Latin Hypercube DOE in GEM-SA. The aircraft and landing gear loads model was then run to provide the corresponding main landing gear component outputs. The outputs of interest are: main fitting *MS* and sliding tube bending moment *MS* at spin-up, spring-back and maximum vertical reaction, as well as internal shock absorber loads such as the upper diaphragm tube *MS* at the maximum compressive upper diaphragm tube load. The sensitivity analysis was carried out in GEM-SA.

For each sensitivity study, the emulator is built on the first 80% of the training data and the accuracy of the emulator is evaluated using the remaining 20% of the training data. Since the emulator calculates a mean function, which passes through the outputs and also quantifies the remaining uncertainty due to the emulator being an approximation of the true model, the emulator accuracy is evaluated graphically using the emulator predictions and their 95% confidence bands, as well as the model output data (data not used in training). Figure 7 shows an example of the emulator accuracy for the main fitting *MS* at spin-up. Generally it was found that the emulators did a reasonable job since the model test data tended to be within the 95% confidence bands of the predictions and errors could be attributed to predicting high values of *MS* since there are fewer training points for the emulator in these regions.

GEM-SA also provides other statistical measures of the emulator accuracy, including 'roughness' values for the input flight parameters, an emulator variance (σ^2) and cross-validation root mean square (RMS) error. The roughness values estimate the smoothness of the model inputs and describes how quickly the output responds to changes in each input[16]. Roughness values greater than one indicate non-linear relationships between the inputs and outputs, while roughness values approaching 100 indicate discontinuities and suggest that the emulator is not working. The σ^2 value provides the variance of the emulator after standardising the output and provides a measure of the non-linearity in the emulator[16]. Finally, the cross-validation RMS error is the square root of the mean square error of the emulator predictions at the validation training points[16].

https://doi.org/10.1017/S0001924000010150 Published online by Cambridge University Press

Table 1
Symmetric landing margin of safety emulator accuracy

Flight Parameter	Emulator Roughness Values					
	Main Fitting MS			Sliding Tube Bending Moment MS		Shock Absorber Upper Diaphragm Tube MS
	Spin-Up	Spring-Back	Maximum Vertical Reaction	Spin-Up	Spring-Back	
θ	1.83	2.79	2.81	1.63	0.63	0.10
V_{A_x}	0.05	0.61	0.09	0.03	0.59	0.02
V_{A_z}	3.67	3.61	**11.78**	1.90	1.66	4.84
μ_{long}	**12.98**	**10.87**	6.28	1.27	1.60	0.80
Port SA	0.05	0.09	1.07	0.06	1.09	0.04
tyre	0.28	0.04	1.14	0.39	0.80	2.75
tyre press	0.13	4.30	1.72	3.59	**10.24**	2.84
mass	0.98	1.53	7.35	3.00	2.71	2.81
CG	1.83	0.32	0.82	3.00	0.70	3.00
Fitted Model Parameters						
σ^2	0.38	0.78	0.69	0.29	0.91	0.15
Cross Validation Results						
Cross Validation RMS Error [%]	0.15	0.79	0.93	0.23	2.71	0.09

The statistical measures of the emulator accuracy for the symmetric landing *MS* sensitivity analysis are presented in Table 1. Roughness values for most input parameters are below 10, which indicates that the emulator is a good approximation to the aircraft and landing gear loads model. Roughness values are greater than 10 (shown in bold) for μ_{long} and the outputs spin-up main fitting *MS* (12·98) and spring-back main fitting *MS* (10·87). They are also greater than 10 for V_{A_z} and the output maximum vertical reaction main fitting *MS* (11·78), and for *tyre press* and the output spring-back sliding tube bending moment *MS* (10·24). Roughness values are less than one for V_{A_x}, which reflects the fact that it is not a significant parameter for the *MS* at any location.

The σ^2 values range from 0·15 to 0·91, which means that the flight parameters only moderately deviate from linearity. The RMS errors, which are not normalised, are 0·15, 0·79 and 0·93 for the spin-up, spring-back and maximum vertical reaction main fitting *MS* respectively; 0·23 and 2·71 for the spin-up and spring-back sliding tube bending moment *MS* respectively; and 0·09 for the upper diaphragm tube *MS*. This data indicates that the emulator may be considered a good representation of the aircraft and landing gear loads model.

4.1 Main effects plots

The main effects plots for the analysis show *MS* versus the normalised flight parameters. The lines represent mean main effects values, averaged over variations in the other parameters. They can be thought of as the expected value of the output with respect to one parameter if the true values of the other parameters are known. These plots show which flight parameters the *MS* is significantly sensitive to and the nature of the input/output relationships.

For symmetric landings, the port and starboard MLG give the same results, therefore only the port MLG results are presented. The symmetric landing spin-up and spring-back main fitting *MS* main effects plots show the same trends as the spin-up and spring-back sliding tube bending moment *MS* main effects plots. Therefore, to be concise, only the main fitting *MS* main effects plots for spin-up and spring-back are shown in Figs 8 and 9. The maximum vertical reaction main fitting *MS* tends to have a constant relationship with most flight parameters, therefore the main effects plots are not illustrated, but they are discussed in the following section. The sliding

https://doi.org/10.1017/S0001924000010150 Published online by Cambridge University Press

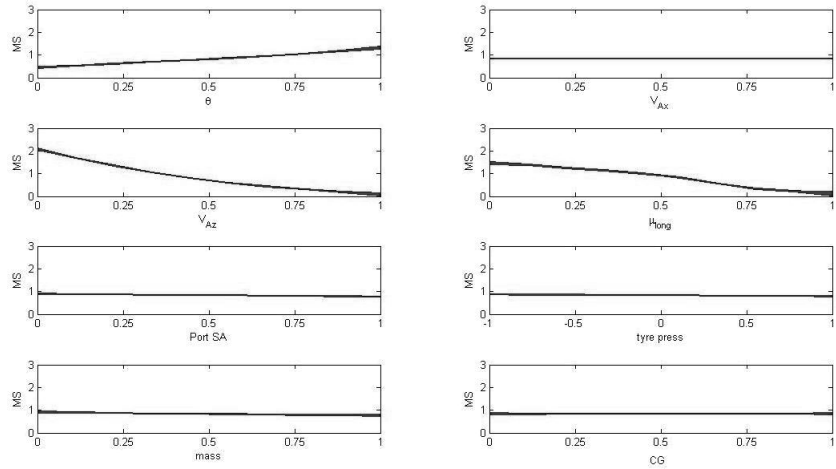


Figure 8. Spin-up main fitting margin of safety main effects plots.

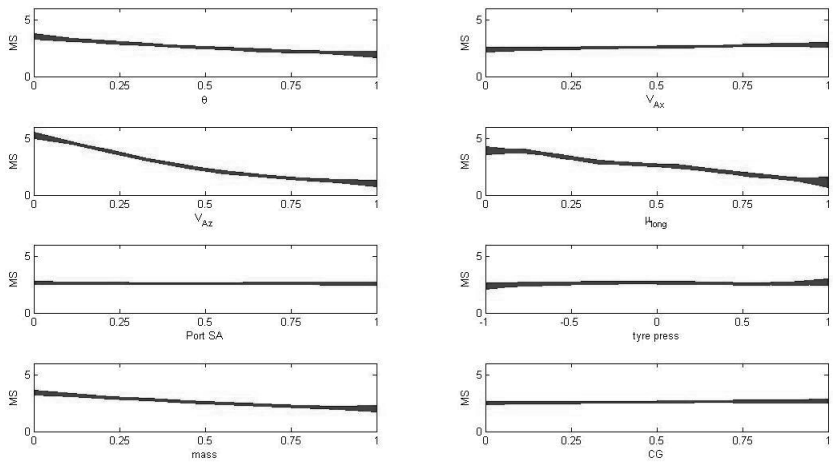


Figure 9. Spring-back main fitting margin of safety main effects plots.

tube bending moment *MS* is only of interest at spin-up and spring-back and therefore it was not considered at the maximum vertical reaction. The symmetric landing main effects plots for the upper diaphragm tube are shown in Fig. 10. The main effects plot for tyre was not illustrated because a discrete uniform distribution was assigned to each tyre type. In GEM-SA, this was described by a continuous distribution and the main effects plots are not meaningful in this case.

4.1.1 Aircraft pitch angle

When the aircraft has a level landing (pitch angle of 0°), the landing gear has a rearward rake angle and due to the vertical and drag force components resolved into landing gear leg-axes, the spin-up drag loads are increased, while the spring-back drag loads are reduced. On the other hand, when the aircraft has a tail-down landing (pitch angle of 13·5°), the landing gear has a forward rake angle and the spin-up drag loads are reduced and the spring-back drag loads are increased.

https://doi.org/10.1017/S0001924000010150 Published online by Cambridge University Press

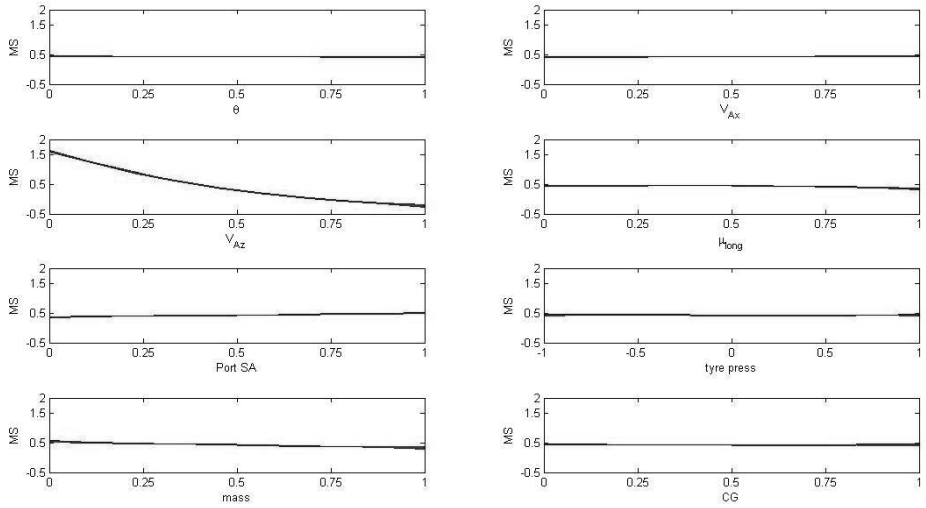


Figure 10. Shock absorber upper diaphragm tube margin of safety main effects plots.

The symmetric landing spin-up main effects plots for the main fitting and sliding tube show that the *MS* increases as θ increases. This is logical considering that the spin-up drag loads are reduced as θ increases. Conversely, the spring-back main effects plots for the main fitting and sliding tube show that the *MS* decreases as θ increases. This also makes sense since the spring-back drag loads are increased as θ increases. At maximum vertical reaction, the *MS* has a constant relationship with θ. The shock absorber upper diaphragm tube *MS* also has a constant relationship with θ and the MEI and TEI, in Section 4.2, show that θ has no significance to the shock absorber upper diaphragm tube *MS*.

4.1.2 Aircraft longitudinal velocity

The flight parameter V_{A_x} has a constant relationship with the spin-up, spring-back and maximum vertical reaction main fitting *MS,* sliding tube bending moment *MS* and shock absorber upper diaphragm tube *MS*. Like θ, the emulator accuracy roughness values are less than one which indicates a linear relationship between V_{A_x} and the *MS* output. The MEI and TEI, discussed in Section 4.2, show that V_{A_x} does not have any significant contribution to the *MS*.

4.1.3 Aircraft vertical descent velocity

For each location, as V_{A_z} increases the *MS* decreases. With increasing V_{A_z}, the vertical and drag axle response loads increase, and therefore this would cause more components to yield and hence the *MS* to decrease.

4.1.4 Longitudinal tyre-runway friction coefficient

Similar to V_{A_z}, with increasing μ_{long}, the vertical and drag axle response loads increase and therefore it is more likely that the component will yield and therefore the *MS* will be less than zero. The flight parameter μ_{long} has a constant relationship with the *MS* for the shock absorber upper diaphragm tube, and the MEI and TEI indicate that it is not as significant.

https://doi.org/10.1017/S0001924000010150 Published online by Cambridge University Press

4.1.5 Main landing gear shock absorber servicing state

While it is understood that an overinflated shock absorber causes higher loads through the landing gear structure and an underinflated shock absorber causes lower loads through the landing gear structure (up to the point of bottoming), the main effects plots for each location show that the *MS* has a constant relationship with the shock absorber servicing state at spin-up, spring-back and maximum vertical reaction. The emulator accuracy values for these flight parameters were also less than one, indicating a linear relationship between the inputs and outputs. The MEI and TEI for *Port SA* are generally low, indicating that they are not significant.

4.1.6 Main landing gear tyre pressure

For each component, the *MS* has a constant relationship with tyre pressure at spin-up, spring-back and maximum vertical reaction. While the MEI, discussed in Section 4.2, do not indicate any significant contributions, the TEI do show that tyre pressure has some significance for the spring-back and maximum vertical reaction main fitting *MS* and the spring-back sliding tube bending moment *MS*.

4.1.7 Aircraft mass and centre of gravity

In components where the *mass* is significant, such as the main fitting and sliding tube bending moment at spring-back and maximum vertical reaction, the *MS* decreases as the mass increases. This is expected since with increasing *mass*, the vertical load increases due to increased kinetic energy and a greater shock absorber gas force, and therefore the *MS* will decrease. For each location, the *MS* has a constant relationship with the *CG* at spin-up, spring-back and maximum vertical reaction.

4.2 Main effects indices and total effects indices

Additional sensitivity analysis data from GEM-SA include the MEI, TEI and First Order Interactions and Higher Order Interactions. MEI represent the contribution of the inputs to the output. A high MEI value means that the variance of the output will be reduced considerably if we learn the true value of the input flight parameter. First Order Interactions, characterise the effect of varying two input flight parameters simultaneously, in addition to the main effects of both parameters. Total Effects Indices (TEI) measure the variance caused by an input and any interaction of any order including that input flight parameter. While an input parameter may have a low MEI, the TEI indicates if its first order and higher order interactions are significant. Table 2 provides the MEI, TEI, First Order Interactions and Higher Order Interactions for the symmetric landing sensitivity analysis. Input flight parameters with MEI and TEI values above 10% are emboldened.

4.2.1 Spin-up

Main Fitting Margin of Safety: For symmetric landings, the MEIs and TEIs indicate that V_{Az}, μ_{long} and θ contribute significantly to the *MS*. The symmetric landing first order interactions account for 6·60% of the main fitting *MS* and the interactions between $\mu_{long} - V_{Az}$ (1·39%), $\mu_{long} - \theta$ (2·48%) and $V_{Az} - \theta$ (1·47%) account for 5·34% of the *MS*.

Sliding tube bending moment margin of safety: Like the main fitting, V_{Az}, μ_{long} and θ are the most significant parameters for the spin-up sliding tube bending moment *MS* MEI and TEI. The sliding tube bending moment *MS* first order interactions between $\mu_{long} - \theta$ (4·26%) and $V_{Az} - \theta$ (1·93%) account for 6·19% of the *MS*.

Findings: The most significant parameters that affect the main fitting and sliding tube bending moment *MS* at spin-up are μ_{long}, V_{Az} and θ.

https://doi.org/10.1017/S0001924000010150 Published online by Cambridge University Press

https://doi.org/10.1017/S0001924000010150 Published online by Cambridge University Press

Table 2
Symmetric port main landing gear *MS* MEI and TEI summarised results

Flight Parameter	Main Fitting MS						Sliding Tube Bending Moment MS				Shock Absorber Upper Diaphragm Tube MS	
	Spin-Up		Spring-Back		Maximum Vertical Reaction		Spin-Up		Spring-Back			
	MEI [%]	TEI [%]	MEI [%]	TEI [%]	MEI [%]	TEI [%]	MEI [%]	TEI [%]	MEI [%]	TEI [%]	MEI [%]	TEI [%]
θ	9.39	**15.24**	4.86	**18.84**	0.22	**21.98**	**22.31**	**30.08**	6.82	**12.26**	0.00	0.22
V_{A_x}	0.00	0.26	0.45	4.10	0.14	1.10	0.25	0.40	0.61	5.64	0.03	0.08
V_{A_z}	**49.78**	**55.19**	**43.85**	**55.98**	**49.23**	**72.81**	**41.67**	**45.27**	**30.55**	**41.06**	**95.56**	**96.80**
μ_{long}	**30.37**	**37.56**	**19.89**	**38.43**	2.16	**28.91**	**24.42**	**30.61**	**31.02**	**41.39**	0.34	1.09
Port SA	0.18	0.41	0.02	0.86	0.18	8.63	0.41	0.66	0.08	6.50	0.43	0.56
tyre	0.09	1.17	0.09	0.47	0.53	8.23	0.12	1.13	0.14	5.28	0.12	1.19
tyre press	0.10	0.52	0.22	10.42	0.22	10.10	0.23	2.17	0.40	**16.07**	0.04	0.92
mass	0.28	2.00	4.75	**13.93**	2.62	**26.29**	0.14	2.00	3.39	**16.71**	1.26	2.33
CG	0.02	1.77	0.10	2.87	0.45	6.34	0.05	1.88	0.26	5.21	0.01	0.98
First Order Interactions	6.60		11.51		18.95		7.83		10.63		0.89	
Higher Order Interactions	3.19		14.26		25.29		2.57		16.09		1.30	

4.2.2 Spring-back

Main fitting margin of safety: The MEI show that μ_{long} and V_{A_z} are the most important parameters for the main fitting *MS*. The TEI show that along with μ_{long} and V_{A_z}, θ, *mass* and *tyre press* are also significant. The first order interactions account for 11·51% of the *MS*. In symmetric landings, the interactions between $\mu_{long} - V_{A_z}$ (1·27%), $\mu_{long} - \theta$ (3·58%), μ_{long} –*mass* (1·89%) and $V_{A_z} - \theta$ (1·23%) account for 7·97% of the *MS*.
Sliding tube bending moment margin of safety: The MEIs indicate that μ_{long} and V_{A_z} are the significant parameters on the sliding tube bending moment *MS*. The TEIs show that *mass*, *tyre press*, and θ and their interactions contribute to the *MS*. The first order interactions account for 10·64% of the *MS*. The interactions between $\mu_{long} - V_{A_z}$ (1·14%), μ_{long} – *mass* (2·11%), *tyre press-mass* (1·39%) account for 4·64% of the interactions. The roughness parameter for *tyre press* was high (10·24) for spring-back, which may be a result of the interactions with *tyre press* as indicated by the TEI.
Findings: V_{A_z}, μ_{long} and θ are significant for the main fitting *MS* and sliding tube bending moment *MS* at spring-back. The flight parameters *mass* and *tyre press* also have an influence on the main fitting *MS* and sliding tube bending moment *MS*.

4.2.3 Maximum vertical reaction

Main fitting margin of safety: The MEI shows that V_{A_z} is the most significant parameter, however the TEIs show that μ_{long}, *mass*, θ and *tyre press* are also significant. The first order interactions account for 18·96% of the *MS*. Interactions between μ_{long}–θ (6·42%), μ_{long}–*mass* (2·84%), V_{A_z}–*mass* (1·24%), θ–*mass* (1·09%) and *Port SA-mass* (1·11%) account for 12·7% of the *MS*.
Findings: The most significant parameters for the maximum vertical reaction main fitting *MS* are V_{A_z}, μ_{long}, *mass* and θ. The flight parameter *tyre press* also has an influence on the main fitting *MS*.

4.2.4 Shock absorber upper diaphragm tube margin of safety

The MEIs and TEIs for the symmetric landing upper diaphragm tube *MS* show that V_{A_z} is the most significant parameter and there are no significant interactions.

5.0 SUMMARY OF SIGNIFICANT FLIGHT PARAMETERS

A summary of the significant flight parameters is presented in Table 3. Each parameter significance is rated as *High* (H), *Medium* (M) or *Low* (L). *High* identifies flight parameters that greatly influence the MLG component *MS*, *Medium* identifies flight parameters that have some influence on the MLG component *MS* and *Low* identifies flight parameters that have little or no influence on the MLG component *MS*. The MLG components considered in this study include the main fitting, sliding tube and shock absorber upper diaphragm tube.

6.0 CONCLUSIONS

The purpose of this paper was to investigate the sensitivity of input flight parameters in an aircraft and landing gear loads model to the serviceability of the main landing gear components, calculated as Margin of Safety, for symmetric landings. Here, the MLG components considered included the main fitting, sliding tube and shock absorber upper diaphragm tube. The components were analysed based on the loads at spin-up, spring back and maximum vertical reaction.

https://doi.org/10.1017/S0001924000010150 Published online by Cambridge University Press

Table 3
Summary of the significant flight parameters to the MLG components *MS*

Flight Parameter		Significance (H/M/L)
Aircraft Euler pitch angle	θ	H
Aircraft longitudinal velocity	V_{A_x}	L
Aircraft vertical descent velocity	V_{A_z}	H
Aircraft mass	*mass*	M
Aircraft centre of gravity location	*CG*	H
MLG tyre type	*tyre*	M
MLG tyre pressure	*tyre press*	M
MLG shock absorber servicing state	*Port SA*	L
Longitudinal tyre-runway friction coefficient	μ_{long}	H

From the sensitivity analysis performed, the significant flight parameters to the main fitting *MS*, sliding tube bending moment *MS* and shock absorber upper diaphragm tube *MS* include:

- μ_{long}, V_{A_z} and θ for the main fitting *MS* and sliding tube bending moment *MS* at spin-up.
- μ_{long}, V_{A_z} and θ for the main fitting *MS* and sliding tube bending moment *MS* at spring-back.
- μ_{long}, V_{A_z}, θ and *mass* for the main fitting *MS* at maximum vertical reaction.
- *mass* and *CG* have an influence on the spring-back and maximum vertical reaction main fitting *MS* and, spring-back sliding tube bending moment *MS*.
- V_{A_z} for the upper diaphragm tube at the maximum upper diaphragm tube load.

ACKNOWLEDGEMENTS

The authors would like to thank the following colleagues at Messier-Bugatti-Dowty for their invaluable assistance in the model development and sensitivity study analysis: Laura Collett, Sidney Smith and Andrew Thomas.

The authors would also like to thank Dr Will Becker, at the European Comission Joint Research Centre, for the useful discussions on Bayesian sensitivity analysis theory, as well as Dr Marc Kennedy formally of the Probability and Statistics Department at the University of Sheffield for the use of GEM-SA.

This paper would not have been possible without the financial support of Messier-Bugatti-Dowty and the Knowledge Transfer Partnerships (KTP) program through partnership number 1216. This KTP was funded by the Technology Strategy Board.

REFERENCES

1. SCHMIDT, R.K. and SARTOR, P. *Landing Gear, Encyclopaedia of Structural Health Monitoring*, edited by BOLLER, C., CHANG, F.-K. and FUJINO, Y. Wiley, 2009, pp 1983-1994.
2. REDDICK, H.K. Safe-Life and Damage-Tolerant Design Approaches for Helicopter Structures,Tech. rep, Applied Technology Laboratory, US Army Research and Technology Laboratories, Ft Eustis, Virginia USA.
3. SARTOR, P., BOND, D., STASZEWSKI, W. and SCHMIDT, R.K. Assessment of the value of an overload indication system through analysis of aviation industry occurrence data, *AIAA J Aircr*, 2009, **46**, (5), pp 1692-1705.

https://doi.org/10.1017/S0001924000010150 Published online by Cambridge University Press

4. SALTELLI, A., CHAN, K. and SCOTT, E.M. *Sensitivity Analysis*, Wiley, 2000.
5. OAKLEY, J.E. and O'HAGEN, A. Probabilistic sensitivity analysis of complex models: A Bayesian approach, *J Royal Statistical Society Series B*, 2004, **66**, (3), pp 751-769.
6. WORDEN, K. and MANSON, G. On the Identification of Hysteretic Systems, Part I: Fitness Landscapes and Evolutionary Identification, *Mechanical Systems and Signal Processing*, 2012, **29**, pp 201-212.
7. WRIGHT, J.R. and COOPER, J.E. *Introduction to Aircraft Aeroelasticity and Loads*, Wiley, 2007.
8. MILWITZKY, B., LINDQUIST, D. and POTTER, D. An Experimental Study of Applied Ground Loads in Landing, Tech Rep 1248, NACA, 1955.
9. KENNEDY, M.C., ANDERSON, C.W., CONTI, S. and O'HAGEN, A. Case studies in gaussian process modelling of computer codes, *Reliability Engineering and System Safety*, 2006, **91**, (10-11), pp 1301-1309.
10. KENNEDY, M.C. and O'HAGEN, A. Bayesian calibration of computer models, *J Royal Statistical Society: Series B Statistical Methodology*, 2001, **63**, (3), pp 425-464.
11. SACKS, J., WELCH, W.J., MITCHELL, T.J. and WYNN, H.P. Design and analysis of computer experiments, *Statistical Science*, 1989, **4**, (4), pp 409-435.
12. WORDEN, K. and BECKER, W. On the identification of hysteretic systems, Part II: Bayesian sensitivity analysis and parameter confidence, *Mechanical Systems and Signal Processing*, 2012, **29**, pp 213-227.
13. BECKER, W., OAKLEY, J., SURACE, C., GILI, P., ROWSON, J. and WORDEN, K. Bayesian sensitivity analysis of a nonlinear finite element model, *Mechanical Systems and Signal Processing*, 2012, **32**, pp 18-31.
14. SARTOR, P., WORDEN, K., SCHMIDT, R.K. and BOND, D. Bayesian Sensitivity Analysis of Flight, Parameters in the Development of a Hard Landing Indication System, In Preparation, 2012.
15. KENNEDY, M.C. GEM-SA Homepage, http://ctcd.group.shef.ac.uk/gem.html.
16. PETROPOULOS, G., WOOSTER, M., CARLSON, T., KENNEDY, M.C. and SCHOLZE, M. A Global, Bayesian sensitivity analysis of the 1d simsphere soil-vegitation-atmospheric transfer, SVAT. Model using Gaussian model emulation, *Ecological Modelling*, 2009, **220**, pp 2427-2440.
17. BAYARRI, M., BERGER, J., HIGDON, D., KENNEDY, M., KOTTAS, A., PAULO, R., SACKS, J., CAFEO, J., CAVENDISH, J., LIN, C. and TU, J. A Framework for Validation of Computer Models, Tech rep, National Institute of Statistical Sciences, General Motors, October 2002
18. BECKER, W.J. ROWSON, J., OAKLEY, J., YOXALL, A., MANSON, G. and WORDEN, K. Bayesian sensitivity analysis of a model of the aortic valve, *J Biomechanics*, May 2011, **44**, pp 1499-1506.

https://doi.org/10.1017/S0001924000010150 Published online by Cambridge University Press